3. TURBULENT DIFFUSION IN THERMALLY STRATIFIED FLOWS

3.1 Why Is DNS Needed to Estimate Turbulent Heat and Mass Transfer in Stably Stratified Flows ?

Density-stratified flows often occur in the ocean and in the atmospheric boundary layer. The diffusion of scalar variables such as heat and mass in stratified flows is strongly affected by buoyancy. It is, therefore, of great importance to investigate the effects of buoyancy on heat and mass transfer to predict the turbulent diffusion of scalar quantities in the environment. Extensive studies on buoyancy effects in density-stratified turbulent flows have been done in the past two decades, but complicated problems, such as the counter-gradient scalar transfer under strongly stable stratification and the effects of molecular diffusivity on scalar diffusion, have not been well understood. Therefore, it should be noted that general circulation models (GCMs) involve uncertain submodels for turbulent scalar diffusion in density stratified flows. In particular turbulent diffusion models based on the eddy diffusivities of heat, mass and momentum for stratified oceanic flows should be carefully examined, since diffusion models suitable to atmospheric stratified flows with the low Prandtl number of about 0.7 are generally used for oceanic stratified flows with high Prandtl or Schmidt numbers, without considering the effects of both molecular diffusivity and the different turbulence fields on turbulent heat and mass fluxes.

Counter-gradient heat and momentum transfer was first observed in laboratories by Komori et al. (1983) in a thermally-stratified open-channel water flow with weak shear. Stillinger et al. (1983), Itsweire et al. (1986) and Rohr et al. (1988) also observed counter-gradient mass transfer in linearly salt-stratified grid-generated turbulence. However, the previous studies on homogeneously stratified water flows did not clarify the details of the counter-gradient scalar and momentum transfer mechanism. Komori et al. (1995b) and Komori and Nagata (1996) recently conducted precise measurements of the counter-gradient scalar and momentum fluxes in strongly stratified water flows with high Prandtl or Schmidt numbers and they clarified the mechanism of this transfer under these conditions. Furthermore, Komori and Nagata (1996) indicated a difference between the scalar transfer mechanism between thermally-stratified air and water flows by comparing their results with previous measurements in stratified air flows. To more clearly investigate the effects of molecular diffusivity on diffusion, measurements in both stratified air and water flows with the same flow field are needed. However, it is so difficult to generate the same flow field in both phases in a laboratory. Therefore, DNS is expected to be a practical numerical tool to realize stratified air and water flows with the same flow fields. In this chapter, numerical results for a DNS of stratified air and water flows are discussed.

3.2 Direct Numerical Simulations of Stably Stratified Flows

3.2.1 Numerical procedure

Figure 24 shows the computational domain used by Nagata and Komori (1995) for a DNS. The DNS was carried out for a homogeneously stratified grid-generated flow. Hot and cold fluids were provided separately upstream of turbulence generation grids and a stratified thermal mixing layer was formed behind the grids. The computations were conducted for two fluids with Prandtl numbers of Pr = 0.7 and 5.0 (corresponding to air and water), and for two Reynolds numbers of Re_M = 2,500 and 1,500, based on the grid mesh size M. Three stratified conditions with bulk Richardson numbers of Ri = 0, 0.08 and 0.22 were used.

The governing equations for a thermally stratified flow are given by:

$$\frac{\partial U_i}{\partial x_i} = 0 , \tag{29}$$

$$\frac{\partial U_i}{\partial t} + U_j \frac{\partial U_i}{\partial x_j} = -\frac{\partial P}{\partial x_i} + \frac{1}{\mathrm{Re}_M} \frac{\partial^2 U_i}{\partial x_j \partial x_j} + \delta_{2i} RiT , \tag{30}$$

$$\frac{\partial T}{\partial t} + U_j \frac{\partial T}{\partial x_j} = \frac{1}{\mathrm{Re}_M \mathrm{Pr}} \frac{\partial^2 T}{\partial x_j \partial x_j} , \tag{31}$$

where all quantities are made dimensionless by the grid mesh size, the cross-sectionally averaged velocity, the bulk-averaged density, and the initial temperature difference. The

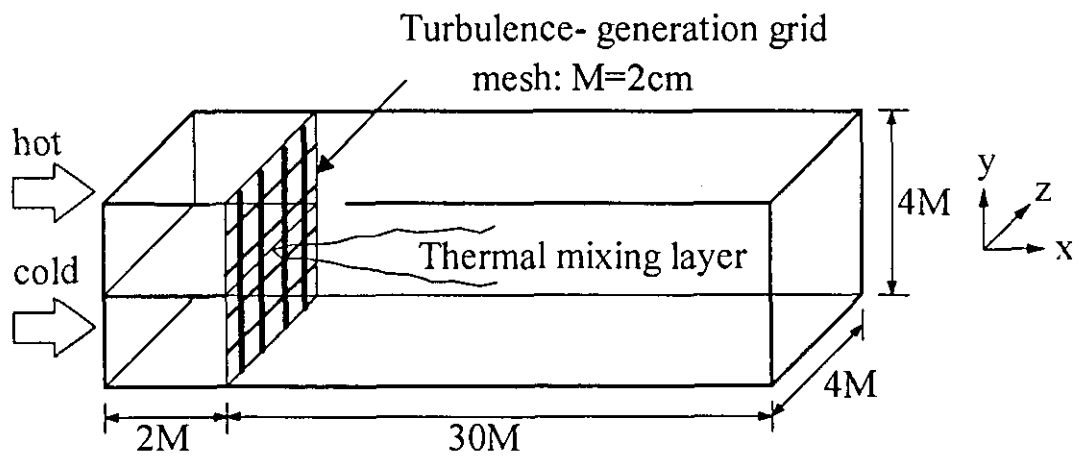

Figure 24. Computational domain used in the DNS for stratified grid-generated turbulence (Nagata and Komori 1995).

governing equations (Eqs.29 ~ 31) were discretized by the same upwind scheme used in the DNS for the sheared air-water interface described in section 3.2 and they were numerically solved by the HS-MAC method.

3.2.2 Test of DNS reliability

640 × 80 × 80 grid points were used in this DNS in the streamwise, spanwise and vertical directions, respectively. The spatial resolution was comparable to the Kolmogorov scale. To examine the accuracy of the DNS, the time-averaged turbulence quantities were computed for a neutrally stratified flow. Figures 25 and 26 show the variations of turbulence intensities and the Reynolds stress in the correlation coefficient form. In the well developed region of $x/M > 4$, the three intensities have almost the same values and they linearly decay in the downstream direction. The Reynolds stress also approaches zero in the region of $x/M >$ 4, confirming that the DNS predicts the grid-generated turbulence well.

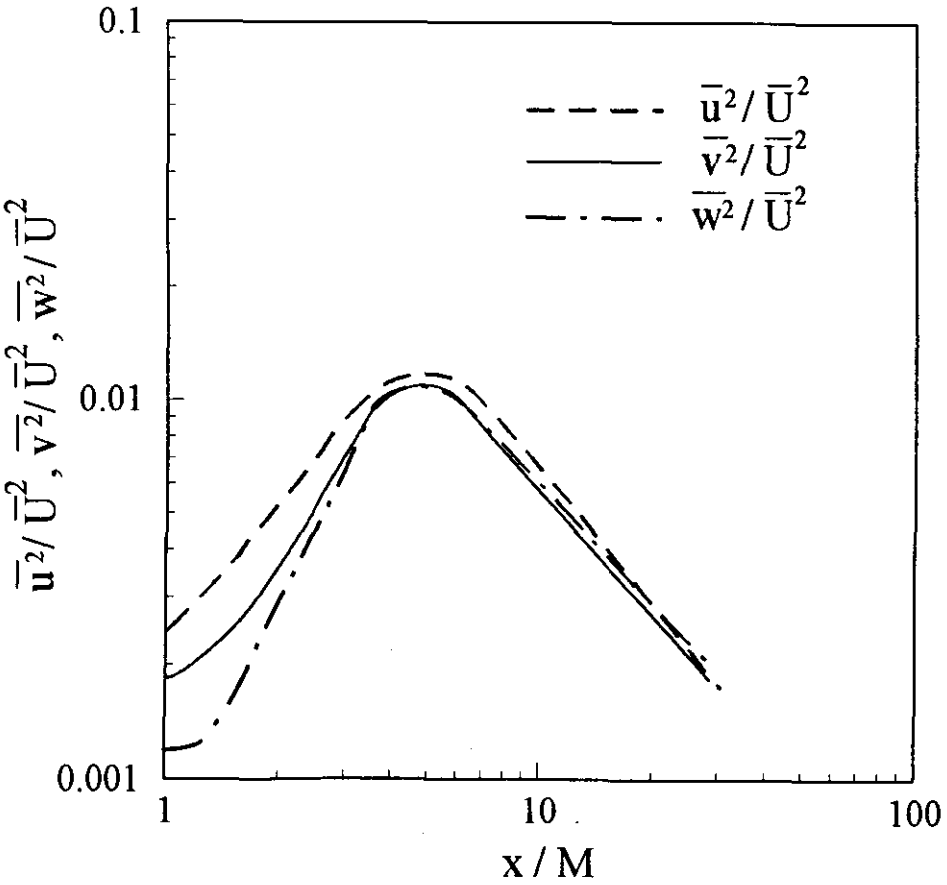

Figure 25. Predictions of turbulence intensities in neutrally stratified grid-generated turbulence (Nagata and Komori 1995).

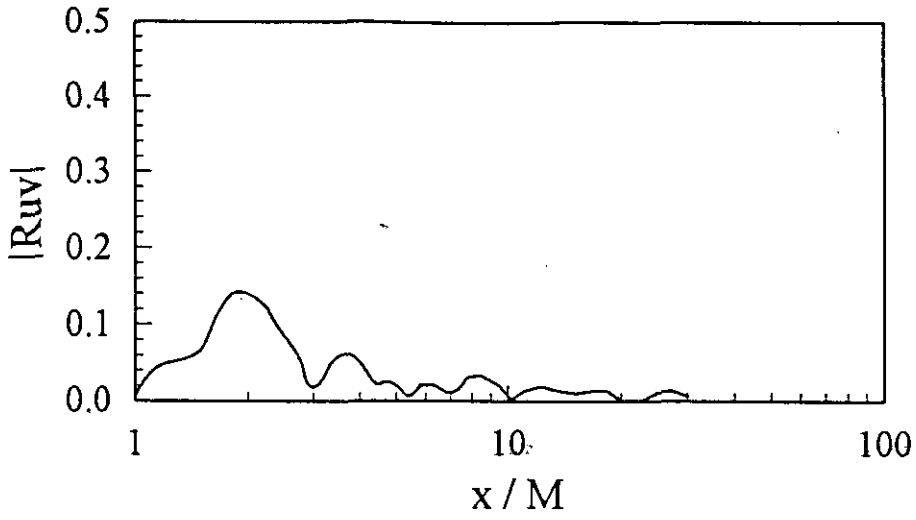

Figure 26. Predictions of the Reynolds stress in neutrally stratified grid-generated turbulence (Nagata and Komori 1995).

3.3 Turbulence Structure and Heat Transfer Mechanism under Strong, Stable Stratification

3.3.1 Counter-gradient heat transfer mechanism in stratified flows

The instantaneous temperature profiles in neutrally (Ri = 0) and stably (Ri = 0.08) stratified air and water flows (Fig.27) clearly show the suppression of heat diffusion by buoyancy. The effect of Prandtl number on diffusion is so remarkable that the enhancement of heat diffusion due to the larger molecular diffusivity of air can be clearly seen.

The turbulent heat flux, $-\overline{v\theta}$, in stratified air (Pr = 0.7) and water (Pr = 5.0) flows (Fig.28) is suppressed with increasing stability and the flux in the water flow changes its sign despite the positive mean temperature gradient in the upward direction. This sign change means that counter-gradient heat transfer occurs in strongly stratified water flows with high Prandtl number. However, for low Prandtl number flow, such counter-gradient heat transfer does not occur as long as the stability is not extremely strong. This finding has also been confirmed by experiments (Komori and Nagata 1996).

To investigate the counter-gradient heat transfer mechanism, the joint probability density function (pdf) of vertical velocity fluctuation, v, and temperature fluctuation, θ, was computed for neutrally and stably stratified water flows (Fig.29). Under neutral stratification where the down-gradient transfer ($-\overline{v\theta} > 0$) is predominant, the pdf prevails in the second and fourth quadrants, whereas under strong stratification the pdf strengthens almost equally in the first and third quadrants. This distribution means that counter-gradient heat transfer is generated by both upward motion of hot fluid and downward motion of cold fluid (Komori and Nagata 1996).

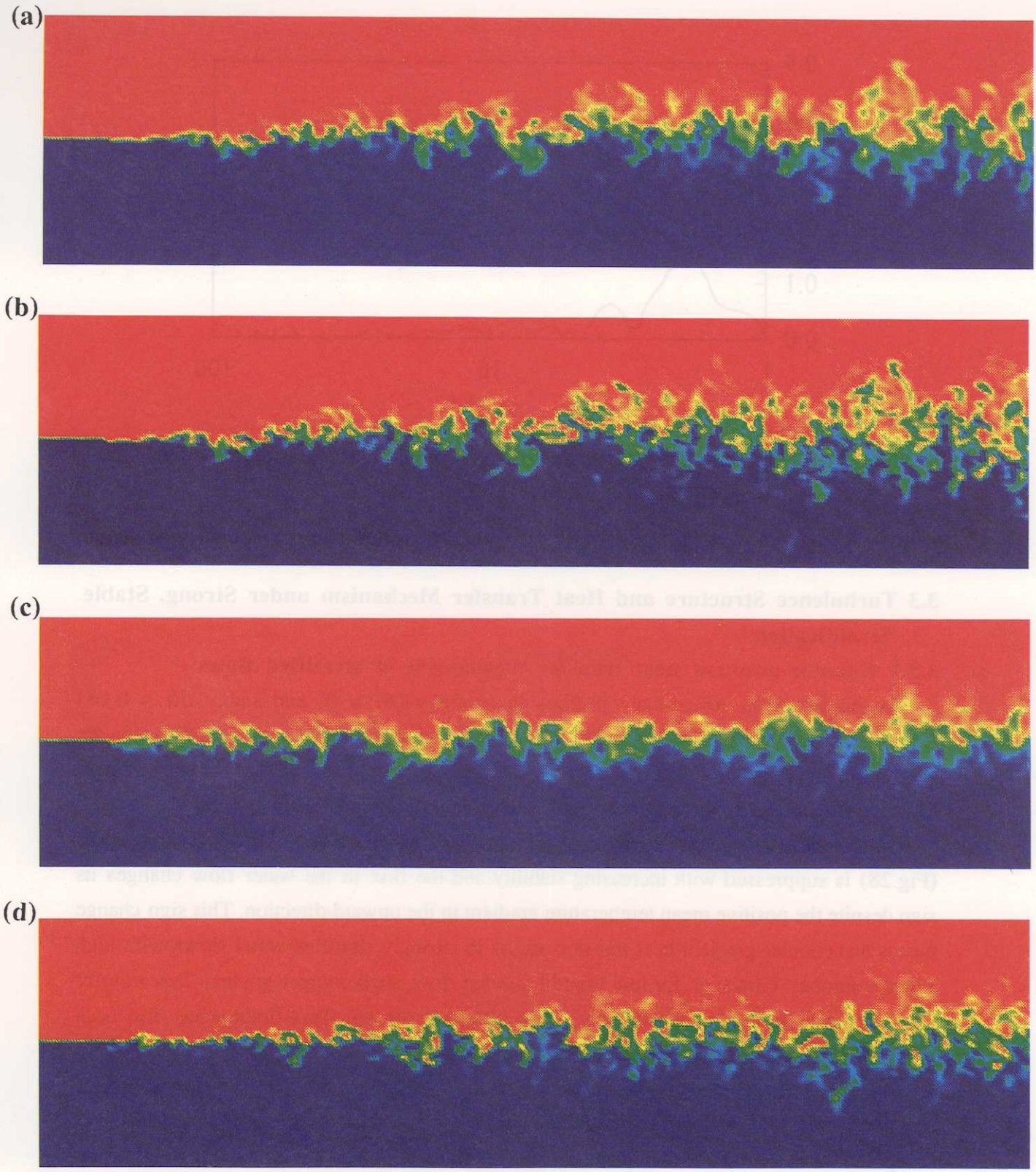

Figure 27. Instantaneous temperature profiles obtained by the DNS for neutrally and stably stratified air and water flows:
(a) in a neutrally stratified air flow (Pr = 0.7 and Ri = 0);
(b) in a neutrally stratified water flow (Pr = 5.0 and Ri = 0);
(c) in a stably stratified air flow (Pr = 0.7 and Ri = 0.08);
(d) in a stably stratified water flow (Pr = 5.0 and Ri = 0.08).

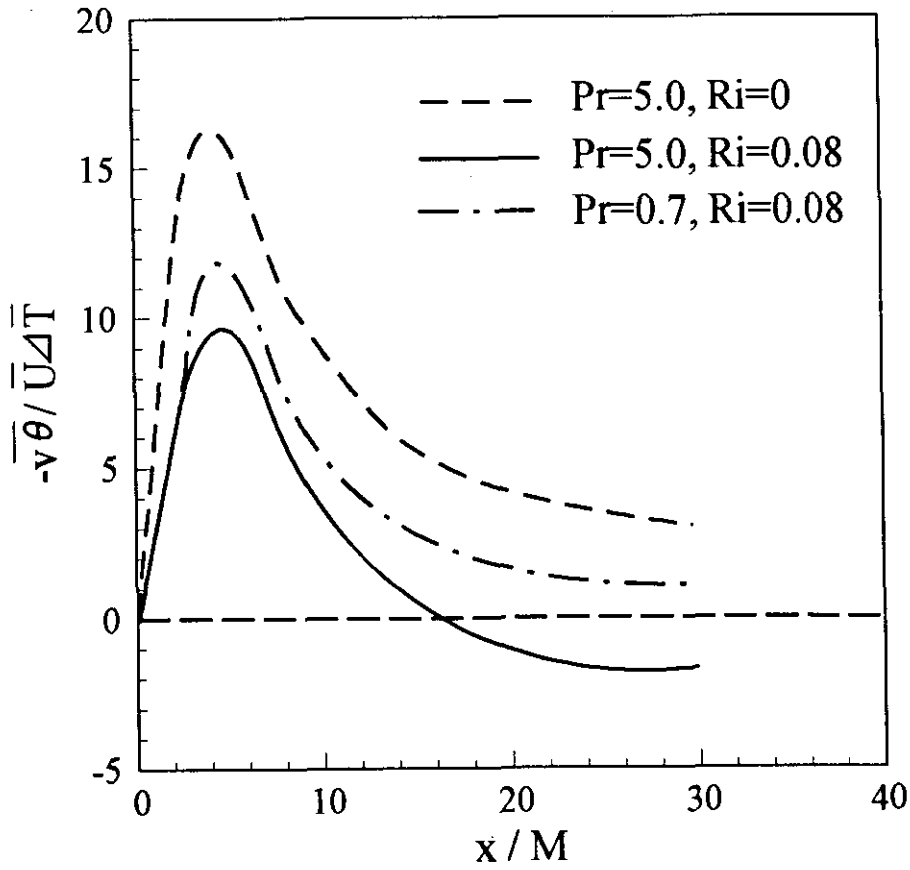

Figure 28. Streamwise distributions of vertical heat flux ($-\overline{v\theta}$) for stratified air (Pr = 0.7) and water (Pr = 5.0) flows (Nagata and Komori 1995).

Thus, it is found that counter-gradient heat transfer under strong stratification is generated by both the upward motion of hot fluid and the downward motion of cold fluid. To know what scale motions contribute to the counter-gradient scalar transfer, the cospectra of v and θ, $Cs_{v\theta}$, were computed at several locations of x/M under neutrally and stably stratified conditions, respectively (Figs.30 and 31; Nagata and Komori 1995). The area under the cospectra multiplied by wave number, k, indicates the amount of heat flux and the negative and positive values of $Cs_{v\theta}$ correspond to down-gradient and counter-gradient heat flux, respectively. Under neutral stratification (Ri = 0), the cospectra at all locations in both air and water flows are always negative for all wave numbers (Fig.30). These negative cospectra show that motions at all scales contribute to down-gradient transfer under neutral stratification. Under strongly stable stratification (Ri = 0.08), the cospectrum starts to change sign for high wave numbers at x/M = 15 in the water flow and the cospectra at x/M > 20 become positive for all wave numbers (Fig.31b). This result means that in the strongly stratified water flow, the small-scale motions first contribute to the counter-gradient transfer. The large-scale motions begin to contribute to the counter-gradient transfer as x/M increases. In the stratified air flow with Ri = 0.08, the counter-gradient heat transfer was not observed

(Fig.31a), but it occurs under extremely strong stratification where $Ri = 0.22$ (Fig.31c).

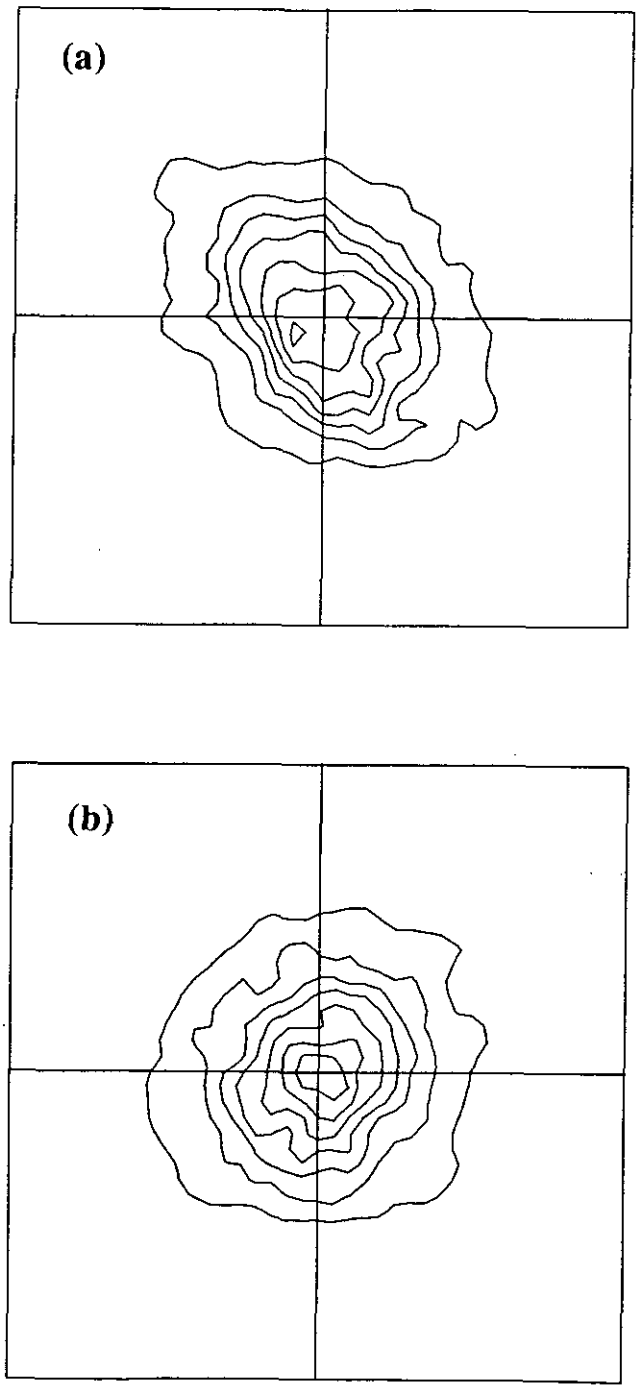

Figure 29. Joint probability density function of vertical velocity and temperature fluctuations in stratified water flows (Nagata and Komori 1995):
(a) under neutral stratification ($Ri = 0$);
(b) under stable stratification ($Ri = 0.08$).

However, this counter-gradient heat transfer is different from that in the water flow, i.e. the counter-gradient transfer is generated only by the large-scale motions in the air flow. The small-motions always contribute to down-gradient transfer in the air flow. These results are in good agreement with previous measurements (Komori and Nagata 1996; Lienhard and Van Atta 1990; Yoon and Warhaft 1990; Jayesh et al. 1991).

Komori and Nagata (1996) summarized the various buoyancy-driven motions in strong stratification illustrated in Figs.29, 30 and 31 as shown in Fig.32. In the initial mixing region, the vertical turbulence kinetic energy (VKE = $\overline{v^2}/2$) in the stably stratified water flow (Ri = 0.08) is larger than or comparable to the available potential energy (APE = $\beta g\overline{\theta^2}/2(\partial\overline{T}/\partial y)$) (Fig.33), and therefore the turbulent motions which are responsible for down-gradient transfer still predominate (Fig.32a). However, the turbulence decays with increasing x/M and the available potential energy becomes rather larger than the turbulence energy. The relative increase in available potential energy first causes the small-scale upward and downward finger-like motions of the low- and high-density fluids, respectively (Fig.32b). These small-scale motions result in the positive cospectra in the high wave number region seen in Fig.31b. In addition to these small-scale motions, large-scale motions are also affected by buoyancy. However, the kinetic energy is still large at large scales in the initial region and therefore the mean flux shows the down-gradient transfer up to the region of x/M=15~20. The large-scale motions begin to contribute to the mean counter-gradient flux as large-scale buoyancy-driven motions further downstream, at x/M > 20 (Fig.32c). This combination generates the positive cospectra values observed throughout the intermediate wave number region in Fig.31(b).

However, the contributions of the small-scale and large-scale motions to the counter-gradient scalar transfer in stratified water flows are quite different from those in stratified air flows as shown in the profiles of the cospectra of v and θ in Fig.31. In stratified air flows with low Prandtl numbers (Pr ≈0.7), counter-gradient heat flux due to small-scale motions have not been seen (Fig.31), because the relative molecular diffusion of heat is rather faster in air than in water as shown in the sketch in Fig.34. In other words, small-scale buoyancy-driven motions cannot be generated in air flows because of the large smearing effect of molecular diffusion. In air, counter-gradient heat transfer occurs only at large scales (Fig.31) and the small-scale motions always contribute to down-gradient transfer, even under strong stratification with a counter-gradient total flux of $-\overline{v\theta} < 0$. Thus, the mechanism of turbulent heat transfer is quite different between stratified air and water flows.

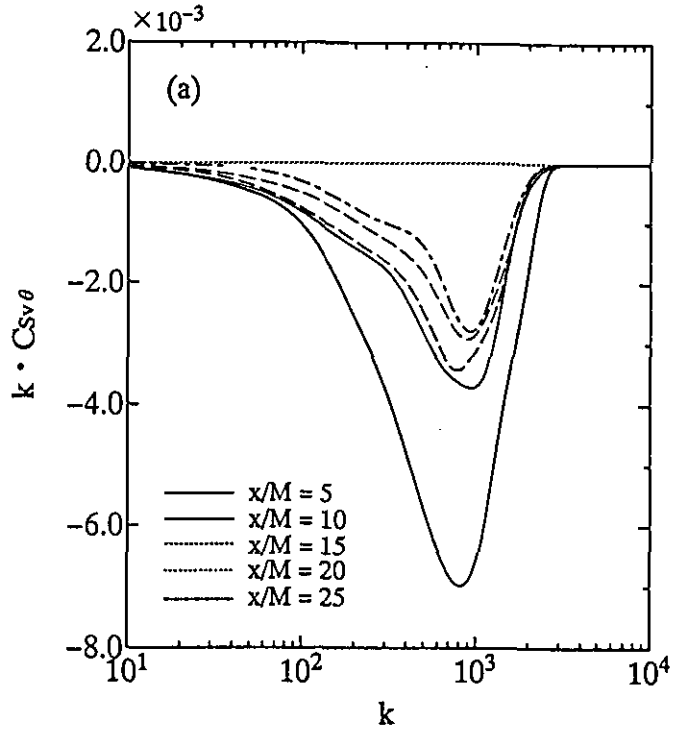

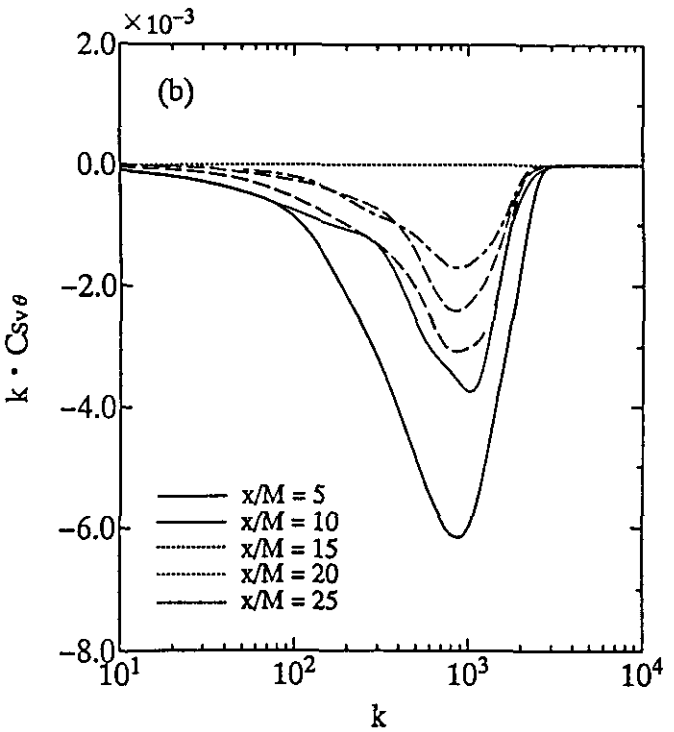

Figures 30. Cospectra of v and θ at several locations of x/M in neutrally stratified air and water flows (Nagata and Komori 1995):
(a) cospectra in the air flow ($Ri = 0$ and $Pr = 0.7$);
(b) cospectra in the water flow ($Ri = 0$ and $Pr = 5.0$).

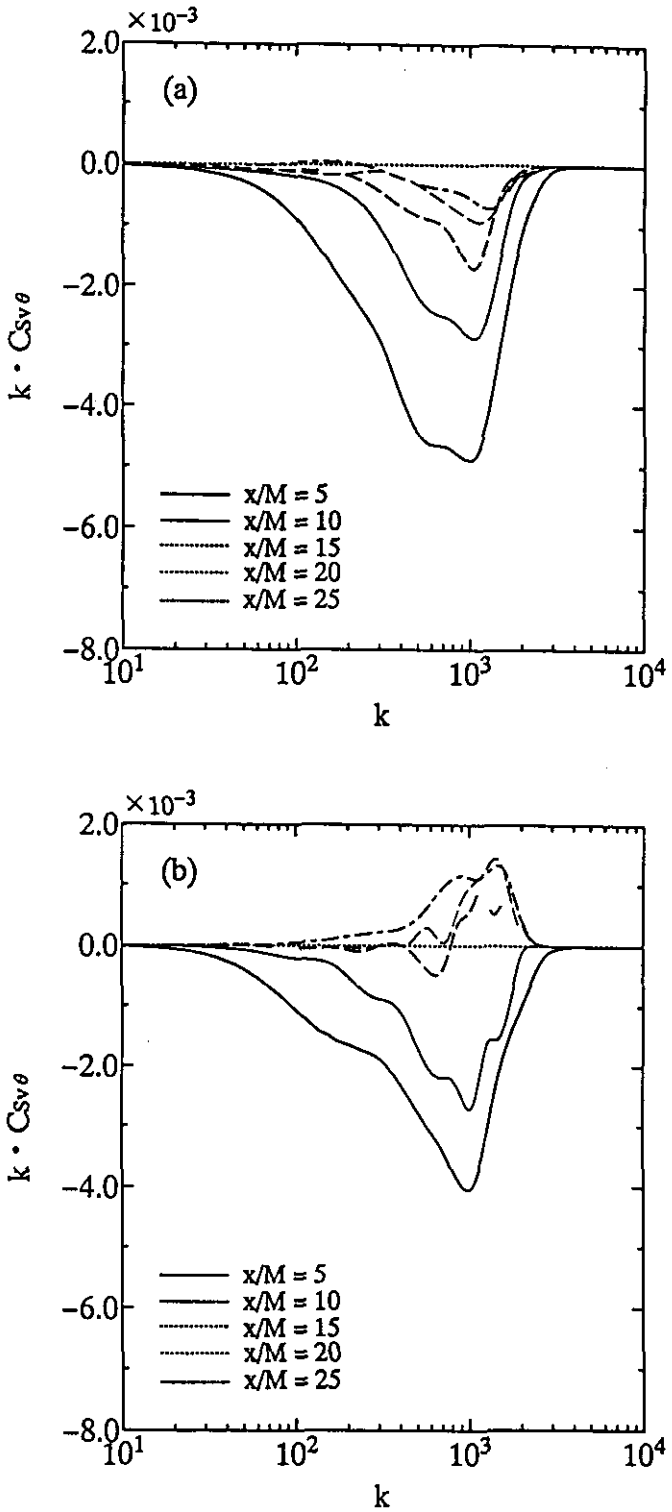

Figure 31. Cospectra of v and θ at several locations of x/M in stably stratified air and water flows (Nagata and Komori 1995):

(a) cospectra in the air flow (Ri = 0.08 and Pr = 0.7);

(b) cospectra in the water flow (Ri = 0.08 and Pr = 5.0).

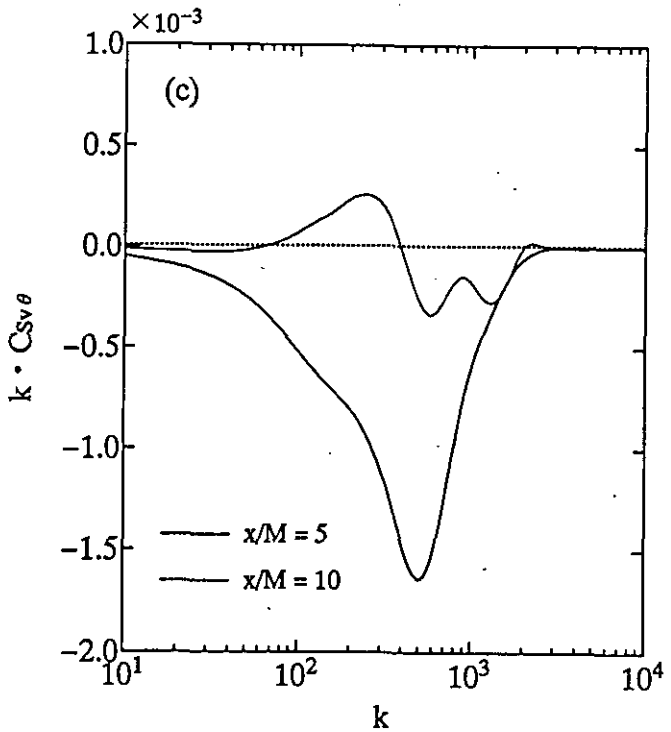

Figure 31. Cospectra of v and θ at several locations of x/M in stably stratified air and water flows (Nagata and Komori 1995):
(c) cospectra in the air flow ($Ri = 0.22$ and $Pr = 0.7$).

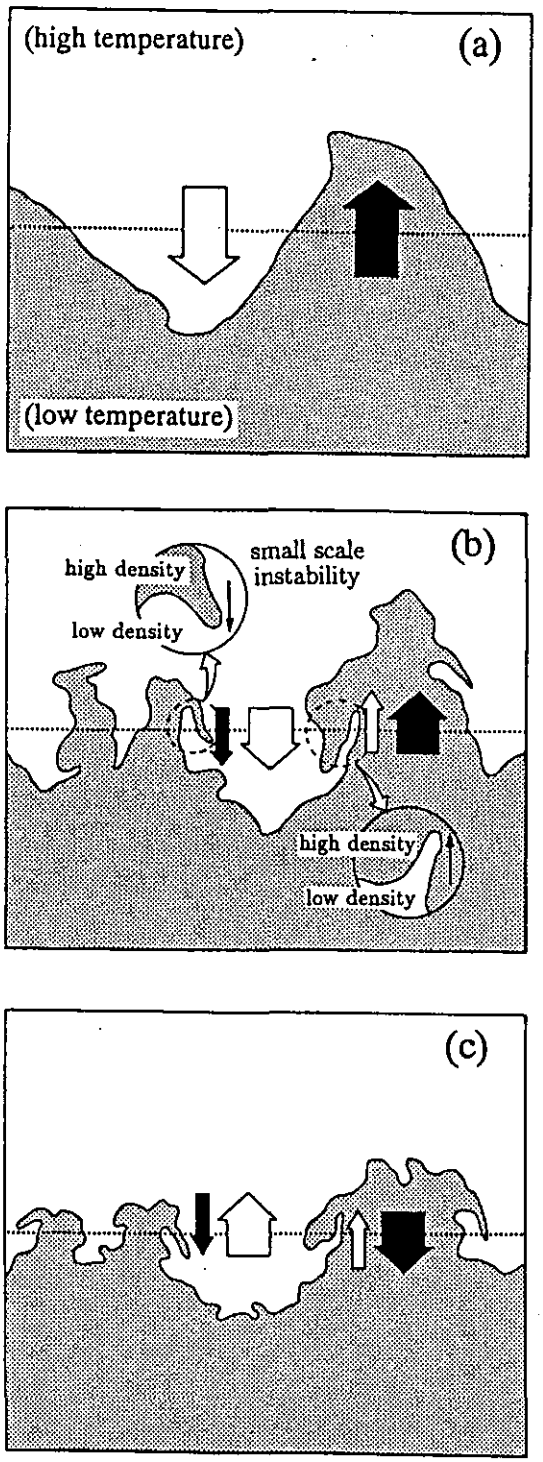

Figure 32. Sketch of buoyancy-driven motions in strongly stratified water flow (Komori et al. 1995b; Komori and Nagata 1996):
(a) $x/M < 10$; (b) $x/M \approx 15$; (c) $x/M > 15$.

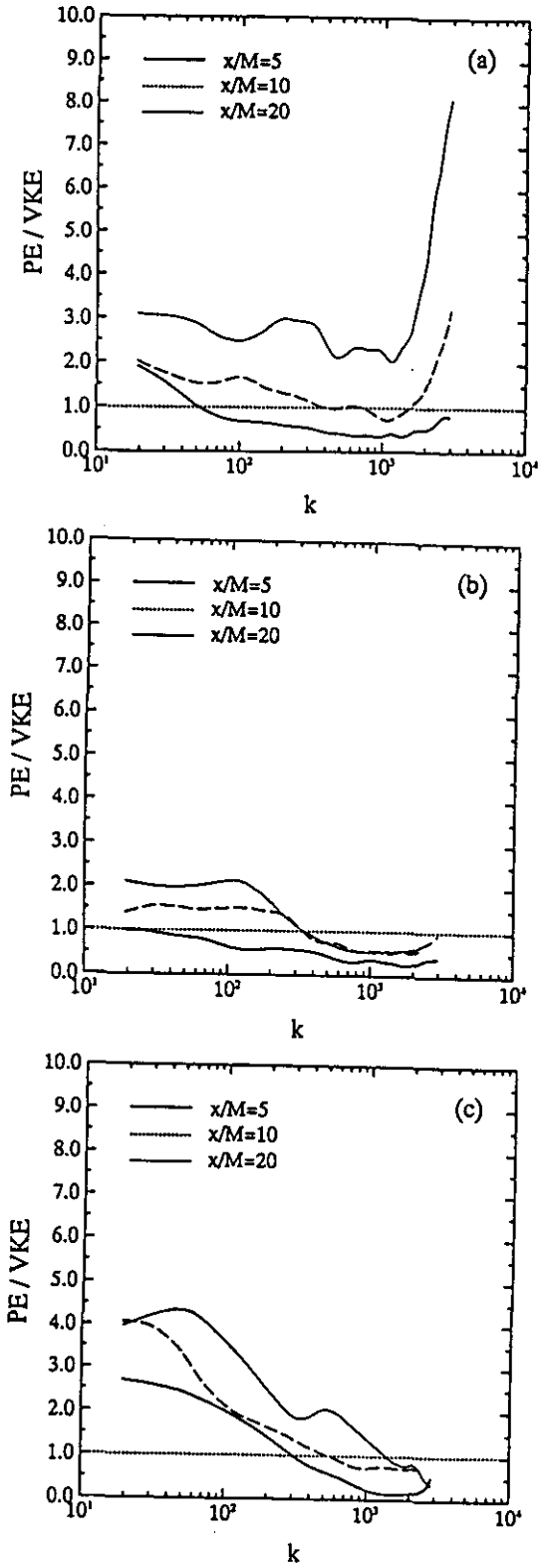

Figure 33. The ratio of vertical turbulence kinetic energy to available potential energy in stably stratified air and water flows (Nagata and Komori 1995):
(a) in the stratified water flow (Ri = 0.08);
(b) in the stratified air flow (Ri = 0.08).
(c) in the stratified air flow (Ri = 0.22)

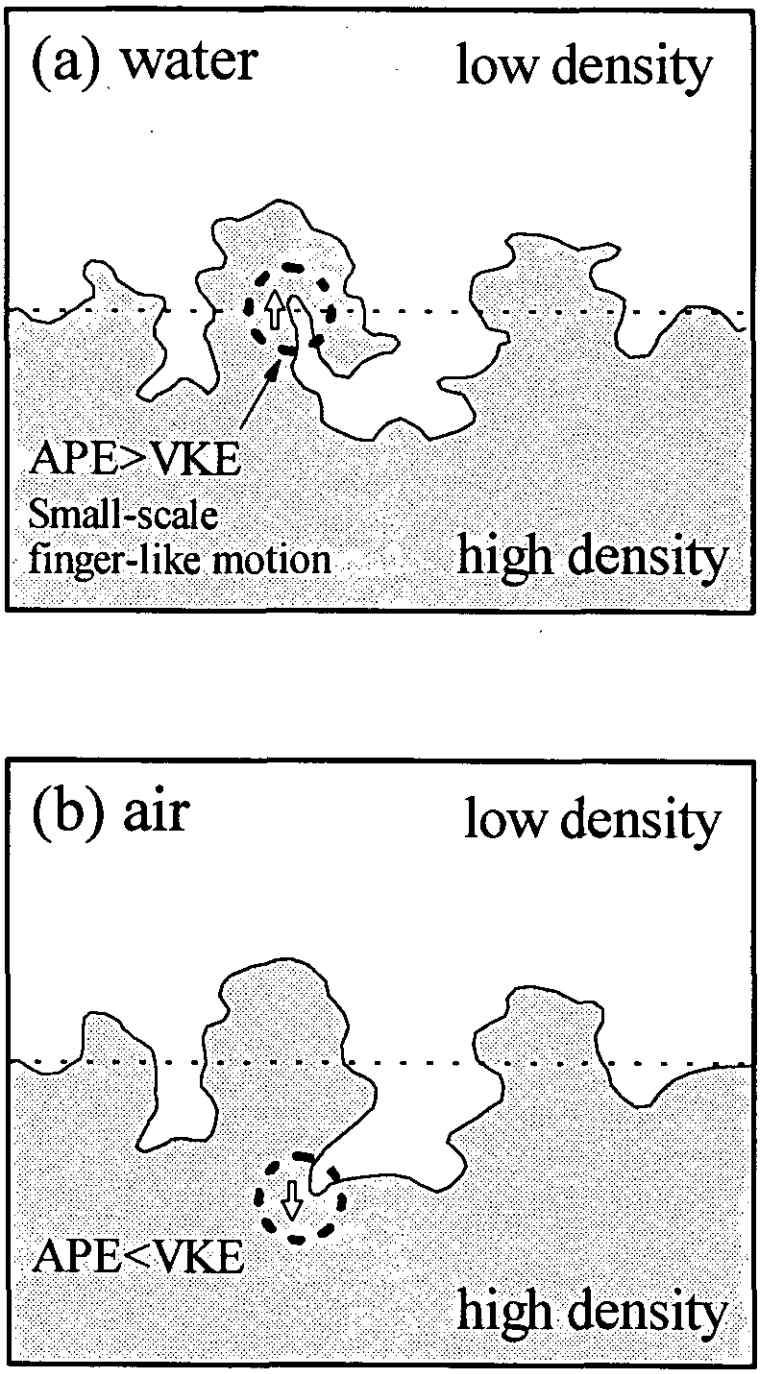

Figure 34. Small-scale motions in stratified water and air flows (Komori and Nagata 1996).
(a) Buoyancy-induced small-scale motions contribute to the counter-gradient heat transfer in a stratified water flow.
(b) Buoyancy-induced small-scale motions are not generated because of the smearing effect of molecular diffusion in a stratified air flow.

3.3.2 The ratio of eddy diffusivity of heat to that of momentum

It is of great importance to investigate the relationship between variations of the eddy diffusivities of heat and momentum with stability in examining scalar and momentum transfer models used in GCMs. The eddy diffusivities of heat and momentum are given in GCMs by functions of the local Richardson number, Ri, and this dependency on Ri is assumed to be the same between atmospheric and oceanic stratified flows. Most of the previous turbulence closure models (e.g. Launder 1975) have shown that the ratio of the eddy diffusivity of heat to that of momentum, K_H/K_M , drastically decreases with increasing Ri for $Ri > 0.1$ (Fig.35), and similar relations between K_H/K_M and Ri have been used in GCMs. However the previous measurements of K_H/K_M are very much scattered among individual studies, while the DNS used by Nagata and Komori (1995) showed slightly decreasing values around 1.7 for both stratified air and water flows. The measurements of Komori and Nagata (1996) also showed behavior similar to that of the DNS. These newer results suggest that Ri is not the only important parameter and that the submodels estimating K_H/K_M in GCMs should be carefully examined for oceanic flows.

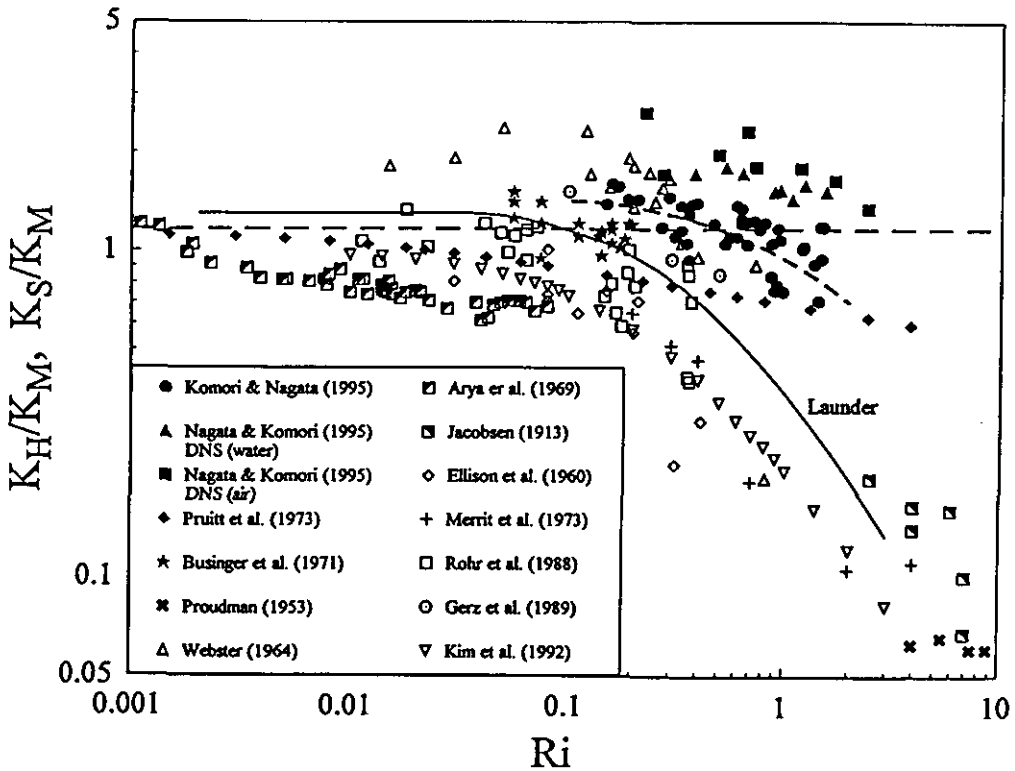

Figure 35. Comparison of the ratio of the eddy diffusivity of heat to that of momentum for the measurements and the predictions generated by DNS.
The filled squares and triangles show the predictions generated by DNS (Nagata and Komori 1995) for stratified air and water flows, respectively, and the filled circles show the measurements by Komori and Nagata (1996). Other symbols show the previous laboratory and field measurements. The solid line shows the predictions by the turbulence closure model of Launder (1975) and the dashed line shows a best-fit curve to the predictions generated by DNS (Nagata and Komori 1995).

4. CONCLUSIONS

Studies on CO_2 transfer across a sheared air-water interface and on turbulent diffusion in thermally stratified air and water flows were conducted using the CGER supercomputer. The results obtained from the studies were reported here.

In the first study, the mechanism of CO_2 transfer across a sheared air-water interface was numerically and experimentally investigated in relation to organized motions in the interfacial region. The main results from the first study can be summarized as follows:

(1) CO_2 transfer across sheared air-water interfaces is intensively promoted by wind shear at wind speeds < 5 m/s, where capillary-like waves are present. However, the CO_2 transfer velocity levels off in the high speed range of 5 m/s < U < 12 m/s, where wind waves are rapidly developing. For wind speeds > 12 m/s, the CO_2 transfer velocity again begins to increase rapidly. Although the behavior of the transfer velocity against wind speed is quite different from those described in previous studies, the effect of wind shear on the mass transfer velocity can be explained by introducing the surface-renewal concept, i.e. the frequency of surface-renewal motions in the water flow.

(2) The organized motions in the air flow over the interface intermittently appear on the fronts of wave crests and there they introduce surface-renewal motions in the water flow through high shear stress acting on the interface. The surface-renewal motions control the mass transfer across wavy sheared gas-liquid interfaces. The generation mechanism of the organized motions and the mass transfer mechanism can be numerically explained by means of direct numerical simulations.

(3) The previous predictions by general circulation models based on the proportional relationship between transfer velocity and wind speed may underestimate the actual CO_2 exchange rate between the atmosphere and the ocean.

The results obtained with DNS in the second study on thermal stratification can be summarized as follows:

(1) Counter-gradient heat and momentum transfer occurs in strongly stratified flows. The counter-gradient transfer is strongly affected by the molecular diffusivity of heat. For stratified water flows, small-scale motions first contribute to this counter-gradient transfer, and then large-scale motions act to generate the counter-gradient heat transfer. The counter-gradient transfer mechanism in water is different from that in stratified air flows with low Prandtl numbers. In stratified air flows, only the large-scale motions contribute to counter-gradient transfer.

(2) The dependency of the ratio of the eddy diffusivity of heat to that of momentum on the local gradient Richardson number is very weak in the homogeneously stratified mixing layer.

(3) The difference between turbulent diffusion in stratified air and water flows should be explicitly modeled in GCMs. The dependency of the eddy diffusivities of heat and